Bioorganic & Medicinal Chemistry Letters 20 (2010) 4831–4835

Contents lists available at ScienceDirect

Bioorganic & Medicinal Chemistry Letters

journal homepage: www.elsevier.com/locate/bmcl

Anti-*T. cruzi* activities and QSAR studies of 3-arylquinoxaline-2-carbonitrile di-*N*-oxides

Esther Vicente [a,b,*], Pablo R. Duchowicz [b], Diego Benítez [c], Eduardo A. Castro [b], Hugo Cerecetto [c], Mercedes González [c], Antonio Monge [a]

[a] *Unidad de Investigación y Desarrollo de Medicamentos, Centro de Investigación en Farmacobiología Aplicada (CIFA), University of Navarra, C/Irunlarrea s/n, 31008 Pamplona, Spain*
[b] *Instituto de Investigaciones Fisicoquímicas Teóricas y Aplicadas, INIFTA (UNLP, CCT La Plata-CONICET), Diag. 113 y 64, C.C. 16, Suc. 4, 1900 La Plata, Argentina*
[c] *Laboratorio de Química Orgánica, Facultad de Ciencias-Facultad de Química, Universidad de la República, Iguá 4225, 11400 Montevideo, Uruguay*

ARTICLE INFO

Article history:
Received 1 May 2010
Revised 17 June 2010
Accepted 19 June 2010
Available online 25 June 2010

Keywords:
Anti-trypanosomal
Chagas disease
Multivariable linear regression
Quinoxaline *N*-oxide
QSAR
Replacement method

ABSTRACT

In a continuing effort to identify new active compounds for combating Chagas disease and other neglected diseases, our research group synthesized and evaluated 23 3-arylquinoxaline-2-carbonitrile di-*N*-oxides against *Trypanosoma cruzi*. Five of them presented IC_{50} values of the same magnitude as the standard drug Nifurtimox, making them valid as new lead compounds. The optimized molecular structures of 23 derivatives represented by 1497 types of DRAGON descriptors were subjected to linear regression analysis, and the derived QSAR was shown to be predictive. In this way, we achieved a rational guide for the proposal of new candidate structures whose activities still remain unknown.

Chagas disease, or American trypanosomiasis, is one of the most important parasitic diseases in Latin America, mainly, in rural areas where poverty is widespread. It is caused by the haemoflagellate protozoan *Trypanosoma cruzi*, which is transmitted to humans by blood-sucking reduviid bugs (*Triatoma infestans* and *Triatoma rubrovaria*) that deposit their infective feces on the skin at the time of biting. Cases have also been reported in the USA and Canada, as a result of transfusion-related infection. Currently, there are an estimated 16–18 million persons infected by *T. cruzi*. Approximately 2–3 million individuals develop the typical symptoms of Chagas disease and some 100 million persons (25% of the Latin American population) are at risk of acquiring this infection.[1] It is estimated that 14,000 people die from the disease every year; this number of deaths in Latin America is greater than that of any other parasite-born disease, including malaria.[2]

This disease represents a serious public health problem in the countries and areas where it is endemic (21 countries in Central and South America) because, in addition to the fact that no effective methods of immunoprophylaxis currently exist, chemotherapy treatment for controlling this parasitic infection remains undeveloped.[1] Nifurtimox and Benznidazol are drugs that are commonly used to treat this disease; however, these compounds produce several adverse reactions and are not effective in the chronic phase of the disease. Therefore, the design, synthesis, and biological evaluation of new compounds with potential activity against *T. cruzi* is considered to be of great importance.[3]

Chagas disease is included in the collective 'neglected diseases' because it principally affects poor people in developing countries for which health interventions (as well as drug research and development) are inadequate to the existing needs.[4–6] In order to be useful worldwide, antichagasic drugs must be inexpensive so that they are routinely available to populations in need in developing countries. Therefore, our research group carried out a search for inexpensive, available reagents so as to be able to prepare new and inexpensive anti-*T. cruzi* drug candidates.

Quinoxalines and their mono- and di-*N*-oxide derivatives display a broad range of biological activities,[7] and quinoxaline di-*N*-oxides are known to undergo bioreductions under hypoxia, causing DNA damage.[8–11] Given the known activity of other classes of bioreductive agents, such as Nifurtimox,[12] it seemed logical to us to evaluate our group of structures against *T. cruzi*. As a result of the anti-Chagas research project, our group published several articles in which the synthesis and biological evaluation of a large amount of quinoxaline and quinoxaline di-*N*-oxides have been described. From these studies, several derivatives, with different patterns of substituents at the quinoxaline nucleus, were prepared with outstanding in vitro anti-trypanosomal activity (i.e., lead

* Corresponding author. Tel.: +34 948425653; fax: +34 948425652 (E.V.).
E-mail addresses: estherviccem@gmail.com, cifa@unav.es (E. Vicente).

0960-894X/$ - see front matter © 2010 Elsevier Ltd. All rights reserved.
doi:10.1016/j.bmcl.2010.06.101

compounds **I–IV**, Fig. 1).[13–18] Screening of the in vitro anti-trypanosomal activity of quinoxaline-2-carbonitrile di-*N*-oxide derivatives[14,18] indicated that their potency mainly depended on the substituents in R^6/R^7 positions, with 6/7-halogenated derivatives being the most active compounds (**I–IV**, Table 1), and on the compounds lipophilicity, with the most active derivatives being the less hydrophilic (Table 1). Recently, we have theoretically demonstrated that quinoxaline di-*N*-oxide could be bioreduced into the parasite, thereby producing reactive species which cause death of the parasite.[19]

In a continuing effort to identify new active compounds to combat Chagas disease, and other neglected diseases,[20–22] our research group prepared 23 3-arylquinoxaline di-*N*-oxide derivatives, **1–23**. Several structural modifications were introduced at the lead compounds **I–IV**, by applying the isosteric and homologous strategies (Fig. 1) attempting to increase the compounds lipophilic properties. Based on the above, we proposed, as a first approximation, the elimination of nonaromatic moiety linked to C-3 of the quinoxaline scaffold (piperazinyl ring in **I–II** or carbonylamino group in **III–IV**), keeping the carbonitrile group linked to C-2, in order to obtain a series of 3-arylquinoxaline-2-carbonitrile di-*N*-oxides, **1–23**. Variations on the electronic profile of the W *para*-substituent of the phenyl moiety were carried out (**1–12**). On the other hand, the halogen atoms present in the prototypes **I–IV** were isosterically replaced by other monovalent groups. These modifications were conducted in order to establish the contributions of electronic and steric parameters for the optimization of the previous lead compounds, **I–IV**.

The 3-arylquinoxaline-2-carbonitrile di-*N*-oxides were obtained by the classical Beirut reaction.[23] The aforementioned compounds (**1–23**) were prepared, in good to excellent yields, according to the synthetic process previously reported.[20,21] Structures of the compounds were confirmed by infrared spectroscopy, nuclear magnetic resonance and mass spectrometry; purity was established by elemental analysis (Scheme 1).

Anti-*Trypanosoma cruzi* activities were determined according to the previously described method.[14,18,24] The existence of the epimastigote form of *T. cruzi* as an obligate mammalian intracellular stage has been revisited and confirmed.[25,26] Moreover, good correlation was observed between the anti-proliferative epimastigote activity and the in vivo anti-*T. cruzi* activity.[27–30] Table 2 shows the results expressed as percentage of epimastigotes *T. cruzi*, Tulahuen 2 strain, growth inhibition (PGI) at 25 μM doses and the corresponding IC_{50} values. As shown in Table 2, almost all of the compounds were active, with PGI >50%, in the preliminary assay at 25 μM. Five of these derivatives (**8**, **11**, **12**, **21**, and **23**) displayed IC_{50} values of the same order than the standard drug Nifurtimox (Nfx), when tested in vitro against epimastigote forms of *T. cruzi*, making them new, valid lead compounds.

Table 1
In vitro activity of previous lead compounds, **I–IV**[a,b] against epimastigote Tulahuen 2 strain of *T. cruzi*

Compound	PGI[c,d] (%)	IC_{50}[e] (μM)	*MLOGP*[f]
I	100	6.5	1.912
II	94	6.7	2.987
III	53.1	19.2	0.868
IV	92.4	10.8	1.616

[a] For structure see Figure. 1.
[b] From Refs. 8,12.
[c] Percentage of growth inhibition respect to untreated parasite.
[d] Inhibition of epimastigotes growth of Tulahuen 2 strain, doses = 25 μM.
[e] Fifty percentage inhibitory concentrations (μM).
[f] Moriguchi-octanol/water partition coefficient.

Some interesting structure–activity relationships can be observed from these results. The most lipophilic compound, **8** (Table 2), according to Moriguchi-octanol/water partition coefficient,[31] was one of the best anti-*T. cruzi* agents. However, in general, the elimination of piperazinyl ring linked to C-3 of the quinoxaline subunit, present in the prototypes **I** and **II**, leads to compounds which do not improve the anti-trypanosomal activity. On the other hand, the elimination of carbonylamino group linked to C-3 of the quinoxaline scaffold, present in the prototypes **III** and **IV**, leads to the most active derivative of both of these series of compounds (**21**, Table 2).

With the aim of completing the analysis of these biological results, we resorted to the quantitative structure–activity relation-

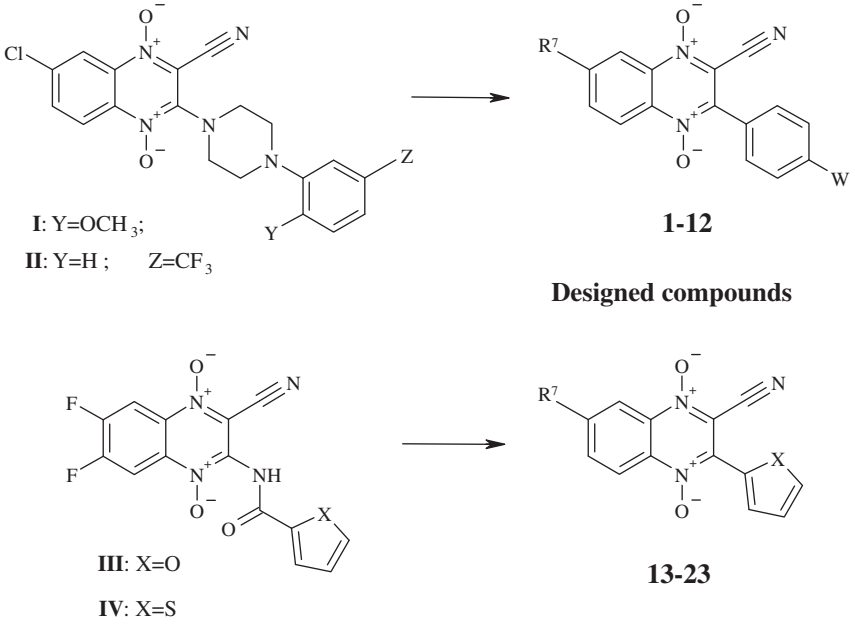

Figure 1. Design of 3-arylquinoxaline-2-carbonitrile di-*N*-oxides, **1–23**, as anti-trypanosomal drugs, obtained from previous lead compounds with structural modifications.[14,18]

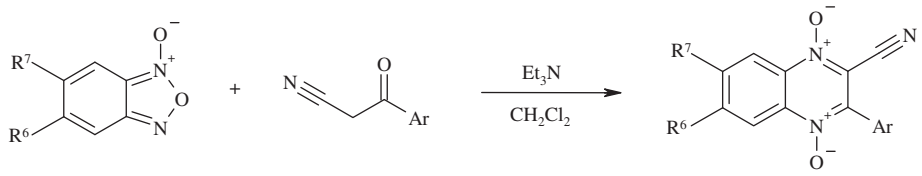

Scheme 1. Synthetic route of 3-arylquinoxaline-2-carbonitrile di-*N*-oxides.[20,21]

Table 2
Structures and in vitro activity of evaluated 3-arylquinoxaline-2-carbonitrile di-*N*-oxides, **1–23** against *T. cruzi*

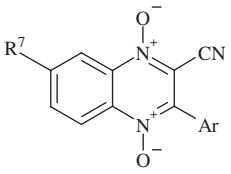

Compound	R^7	Ar	PGI[a,b,c] (%)	IC_{50}[c,d] (μM)	*MLOGP*[e]
1	F	Phenyl	89.4	15.4	2.230
2	CF_3	Phenyl	100	15.1	2.716
3	H	4′-Fluorophenyl	82.8	15.2	2.230
4	F	4′-Fluorophenyl	63.8	14.4	2.622
5	CF_3	4′-Fluorophenyl	100	14.9	3.103
6	OCH_3	4′-Fluorophenyl	84.2	14.6	1.972
7	F	4′-Chlorophenyl	85.4	13.4	2.744
8	CF_3	4′-Chlorophenyl	100	9.2	3.219
9	H	4′-Trifluoromethoxyphenyl	100	14.5	1.944
10	F	4′-Trifluoromethoxyphenyl	80.2	13.1	2.331
11	CF_3	4′-Trifluoromethoxyphenyl	100	9.2	2.790
12	OCH_3	4′-Trifluoromethoxyphenyl	100	8.2	1.688
13	H	2′-Furyl	46.3	25.0	0.582
14	F	2′-Furyl	83.4	14.9	0.983
15	Cl	2′-Furyl	64.5	18.9	1.113
16	CH_3	2′-Furyl	68.5	18.1	0.845
17	CF_3	2′-Furyl	100	12.5	1.495
18	OCH_3	2′-Furyl	33.4	>25.0	0.354
19	H	2′-Thienyl	100	12.7	1.354
20	F	2′-Thienyl	100	13.0	1.755
21	Cl	2′-Thienyl	100	7.1	1.885
22	CH_3	2′-Thienyl	74.3	14.8	1.617
23	CF_3	2′-Thienyl	100	7.8	2.267
Nfx[f]	—	—	100	7.7	−0.746

[a] Percentage of growth inhibition with respect to untreated parasite.
[b] Inhibition of epimastigotes growth of Tulahuen 2 strain, doses = 25 μM.
[c] The results are the means of three different experiments with a SD less than 10% in all cases.
[d] Fifty percentage inhibitory concentrations (μM).
[e] Moriguchi-octanol/water partition coefficient.
[f] Nifurtimox.

ships (QSAR) theory for elucidating the regularities present in data.[32,33] The ultimate role of this theory is the proposal of a model capable of estimating the activities of compounds by relying on the assumption that these resulting effects are a consequence of the molecular structure. In our study, we further explored the biological profile exhibited by 3-arylquinoxaline-2-carbonitrile di-*N*-oxides, establishing predictive models based on the current experimental data available. We started by analyzing the effect of lipophilicity values on the activity of compounds by means of QSAR models, expressing the lipophilicity contribution with the Moriguchi-octanol/water partition coefficient (*MLOGP*).[31] Next, the molecular structure of the studied 3-arylquinoxaline-2-carbonitrile di-*N*-oxide derivatives, **1–23**, was appropriately represented by 1497 theoretical descriptors, calculated with DRAGON software.[34] These molecular descriptors included definitions of all types, capturing the constitutional, topological, geometrical or electronic aspects of the molecular structures being considered, which were obtained through mathematical formulae obtained from several theories, such as the Chemical Graph Theory, Information Theory, Quantum Mechanics, etc.[35–37] The best structure–activity models were searched by means of the replacement method (RM) variable subset selection technique, an algorithm based on multivariable linear regression analysis.[38,39]

In each reported structure–activity relationship, we developed a model for a set of calibration compounds belonging to the training set, and after that, we corroborated its predictive power by means of predicting the activities on external molecules that were not considered during the fitting of the model and which constitute the test set. Selection of the members for both sets was carried out in such a way that all of the members similar structural characteristics. This table also includes the predictions achieved by Eqs. 1–4, shown below.

We began the QSAR analysis by establishing a relationship between PGI and the lipophilicity of the quinoxaline derivatives, expressed by the Moriguchi-octanol/water partition coefficient (*MLOGP*). The following linear regression was found:

$$\log_{10}\mathrm{PGI} = 1.691(\pm 0.07) + 0.109(\pm 0.03)\cdot MLOGP \quad (1)$$
$$N = 16,\quad d = 1,\quad N/d = 16,\quad R = 0.662,$$
$$S = 0.107,\quad FIT = 0.643,\quad p < 10^{-5}$$
$$\text{range in PGI} : 33.4\text{—}100\%,\ \text{outliers}(> 2S) : 0$$
$$R_{loo} = 0.465,\quad S_{loo} = 0.129,\quad S_{rand} < S,$$
$$N_{val} = 7,\quad R_{val} = 0.610,\quad S_{val} = 0.097$$

In this equation, N corresponds to the number of compounds, R is the coefficient of correlation, S stands for the model's standard deviation of calibration, *FIT* is the Kubinyi parameter,[40] p is the significance of the model, subindex *loo* stands for the Leave-One-Out Cross Validation technique,[41,42] S_{rand} represents the standard deviation obtained according to the Y-Randomization technique,[43] and *val* subindex corresponds to the external validation test set. Whether taking into account calibration or considering validation points, it is clearly observed that Eq. 1 was unable to describe the PGI effect of quinoxaline compounds. It is clearly appreciated that Eq. 1 was unable to describe the PGI effect of quinoxaline compounds, either from the calibration or the validation points of views. Therefore, as a next step, we searched the best one-, two-, and three-variable linear regression models by using the replacement method (RM) approach, which was able to select the most relevant and representative structural descriptors for the training set. This exploration led to the following two-variable model:

$$\log_{10}\mathrm{PGI} = 5.9(\pm 0.5) - 0.040(\pm 0.009)\cdot RDF080u - 22(\pm 3)\cdot G1e \quad (2)$$
$$N = 16,\quad d = 2,\quad N/d = 8,\quad R = 0.898,$$
$$S = 0.065,\quad FIT = 2.720,\quad p < 10^{-5}$$
$$\text{range in PGI} : 33.4\text{—}100\%,\ \text{outliers}(> 2.5S) : 0$$
$$R_{loo} = 0.853,\quad S_{loo} = 0.086,\quad S_{rand} = 0.079,\quad R_{max} = 0.497$$
$$N_{val} = 7,\quad R_{val} = 0.479,\quad S_{val} = 0.083$$

where R_{max} is the maximal intercorrelation between the descriptors participating in Eq. 2, revealing that there is no serious duplication of information of the descriptors.

Table 3
Predicted biological data of 3-arylquinoxaline-2-carbonitrile di-*N*-oxides, **1**–**23**, according to QSAR equations (1)–(4)

Compound	PGI[a] (%)	PGI[b] (%)	IC_{50}[c] (μM)	IC_{50}[d] (μM)
1*	85.9	82.2	13.1	18.1
2	97.0	106.9	11.3	13.0
3	85.9	92.4	13.1	18.1
4	94.7	77.9	11.6	15.3
5	106.9	101.4	10.0	12.1
6*	80.5	105.8	14.3	14.3
7	97.7	82.0	11.2	13.2
8*	110.0	106.7	9.6	9.9
9*	79.9	88.7	14.4	10.8
10	88.1	74.9	12.7	10.2
11	98.8	92.5	11.0	9.2
12	75.0	91.9	15.6	9.8
13	56.8	64.0	22.0	21.8
14	62.8	71.8	19.4	15.3
15	64.9	72.1	18.7	15.3
16*	60.7	69.8	20.3	20.9
17*	71.4	80.7	16.6	11.5
18	53.7	30.8	23.7	47.4
19	68.9	85.0	17.3	17.3
20	76.2	82.2	15.3	12.2
21*	78.7	86.7	14.6	12.2
22	73.6	79.6	15.9	17.2
23	86.7	96.8	13.0	9.4

[a] PGI predicted according to Eq. 1.
[b] PGI predicted according to Eq. 2.
[c] IC_{50} predicted according to Eq. 3.
[d] IC_{50} predicted according to Eq. 4.
* Data used as test set.

This QSAR had predictive capability and acceptably predicted the test set compounds (see Table 3). *RDF*080*u* is the Radial Distribution Function 8.0/unweighted, while *G*1*e* is the first component symmetry directional WHIM index/weighted by atomic Sanderson electronegativities.[44] Both of them are highly conformational dependent structural attributes and are suitable for complex-behaving properties because they take into account the 3D-arrangement of the atoms without ambiguities (as those appearing when using chemical graphs), and also because they do not depend on the molecular size, thus being applicable to a large series of molecules posing great structural variance; the descriptors are common characteristics to all of the molecules modeled. The Radial Distribution Function *RDF*080*u* is a kind of molecular descriptor defined for an ensemble of atoms, and may be interpreted as the probability distribution for finding an atom in a spherical volume of certain radius, incorporating different types of atomic properties in order to differentiate the nature and contribution of atoms to the property being modeled. In the case of *RDF*080*u*, the sphere radius is 8.0 Å and no atomic property is used, thus solely characterizing the molecular size. The WHIM descriptor *G*1*e* is calculated based on statistical indices of the atoms projected onto three principal axes (principal components) obtained from weighted covariance matrices of the atomic coordinates. The weights used are again the atomic properties that enable differentiation among atoms. The aim of defining such indices is to capture 3D-information regarding size, shape, symmetry, and atom distributions with respect to invariant reference frames. Similarly, we have previously stated that electronic characteristic of various groups of *N*-oxide containing heterocycles were fundamental for explaining the anti-*T. cruzi* activity.[19]

We continued the QSAR study by establishing a link between IC_{50} values and the *MLOGP* partitioning coefficients. The following linear regression was found:

$$\log_{10}IC_{50} = 1.4(\pm 0.1) - 0.14(\pm 0.05)\cdot MLOGP \quad (3)$$
$$N = 16,\quad d = 1,\quad N/d = 16,\quad R = 0.604,\quad S = 0.157,$$
$$FIT = 0.472,\quad p < 10^{-5}$$
$$\text{range in } IC_{50} : 7.8\text{—}25,\ \text{outliers}(> 2.5S) : 0$$
$$R_{loo} = 0.351,\quad S_{loo} = 0.086,\quad S_{rand} < S,$$
$$N_{val} = 7,\quad R_{val} = 0.495,\quad S_{val} = 0.156$$

Eq. 3 also had poor quality on this quinoxaline data set. We also searched the best linear regressions through the RM in the pool of 1497 descriptors. The predictive linear QSAR reported in Eq. 4 given by two descriptors was able to capture the essential structural features of the quinoxaline di-*N*-oxide derivatives that related to their anti-trypanosomal effect.

$$\log_{10}IC_{50} = -0.9(\pm 0.7) - 4.5(\pm 1)\cdot SIC0 + 22(\pm 3)\cdot G1e \quad (4)$$
$$N = 16,\quad d = 2,\quad N/d = 8,\quad R = 0.924,\quad S = 0.078,$$
$$FIT = 3.816,\quad p < 10^{-5}$$
$$\text{range in } IC_{50} : 7.8\text{—}25,\ \text{outliers}(> 2S) : 0$$
$$R_{loo} = 0.888,\quad S_{loo} = 0.094,\quad S_{rand} = 0.080,\quad R_{max} = 0.097$$
$$N_{val} = 7,\quad R_{val} = 0.646,\quad S_{val} = 0.144$$

Again, this QSAR resulted capable of predicting quinoxalines that had not been contemplated during the model development. The *SIC*0 topological descriptor corresponds to the structural information content (neighborhood symmetry of 0-order).[44] It measures the complexity of a compound as the diversity of elements present in its molecular structure, such as atoms, bonds, cycles, etc. In this case, *SIC*0 descriptor expresses the zero-order neighborhood symmetry for all of the vertexes in the chemical graph.

Models from the QSAR Theory enable us to predict the activity for substances that have yet not been tested due to the fact that they are

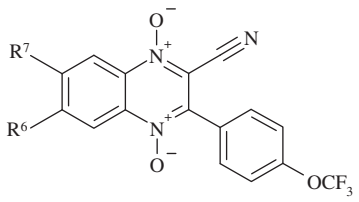

46, R^6=H; R^7=Cl, predicted IC_{50}=8.3 μM

64, R^6=F; R^7=F, predicted IC_{50}=9.9 μM

65, R^6=Cl; R^7=Cl, predicted IC_{50}=7.2 μM

Figure 2. Structures of the three best resulting anti-trypanosomal derivatives, as predicted by QSAR equations 2 and 4, among the 49 newly proposed 3-arylquinoxaline-2-carbonitrile di-*N*-oxides.[45]

unstable or simply because their measurement requires too much time or is costly. In terms of economical aspects, these studies permit rational use of the resources available in the laboratory, avoiding the need to perform expensive and unnecessary experimental determinations. With respect to moral aspects, QSAR applied to the field of Medicinal Chemistry have reached a great importance in the virtual screening of new compounds before their synthesis, and thus represent an effective alternative that reduces animal testing in biological assays. Application of the QSAR equations developed in this work now enables one to propose new candidate structures that still do not have experimentally assigned biological data.

In view of the results achieved and in a further attempt to improve the biological profile of these quinoxaline di-*N*-oxide, we applied the QSAR models that we developed in order to estimate the anti-trypanosomal parameters of new possible antichagasic candidates that still do not present experimentally assigned biological data. The new molecular structures were proposed on the basis that these chemicals can be synthesized from inexpensive and commercially available reagents.

A total of 49 different structures, **24**–**72**, were predicted as anti-trypanosomal candidates, using a model for each evaluated parameter (PGI and IC_{50}). Only four of them showed PGIs less than 50% and IC_{50} values greater than 25 μM, so they are considered to be inactive compounds. Among the other 43 active derivatives, three of them (**46**, **64**, and **65**) are highlighted, showing IC_{50} values less than 10 μM, good enough to justify their synthesis. Figure 2 summarizes the three best resulting anti-trypanosomal structures as predicted by Eqs. 2 and 4. As can observed, these three derivatives showed halogenated atoms at position R^6 and/or R^7 and the group 4′-trifluoromethoxyphenyl linked to the R^4 position of the quinoxaline scaffold.[45]

Acknowledgments

This work has been carried out with the financial support of the RIDIMEDCHAG-CYTED. P.R.D. and E.A.C. are researchers from the National Council of Scientific and Technological Research (CONICET).

Supplementary data

Supplementary data associated with this article can be found, in the online version, at doi:10.1016/j.bmcl.2010.06.101.

References and notes

1. Cerecetto, H.; González, M. *Mini-Rev. Med. Chem.* **2008**, *8*, 1355.
2. Ribeiro, I.; Sevcsik, A.-M.; Alves, F.; Diap, G.; Don, R.; Harhay, M. O.; Chang, S.; Pecoul, B. *PLoS Negl. Trop. Dis.* **2009**, *3*, e484.
3. Rivera, G.; Bocanegra-García, V.; Ordaz-Pichardo, C.; Nogueda-Torres, B.; Monge, A. *Curr. Med. Chem.* **2009**, *16*, 3286.
4. Trouiller, P.; Olliaro, P.; Torreele, E.; Orbinski, J.; Laing, R.; Ford, N. *Lancet* **2002**, *359*, 2188.
5. Caines, K. In *GHP Study Paper 4: Global Health Partnerships and Neglected Diseases*; DFID Health Resource: London, UK, 2004.
6. Croft, S. L. *Curr. Opin. Investig. Drugs* **2007**, *8*, 103.
7. Carta, A.; Corona, P.; Loriga, M. *Curr. Med. Chem.* **2005**, *12*, 2259.
8. Chowdhury, G.; Kotandeniya, D.; Daniels, J. S.; Barnes, C. L.; Gates, K. S. *Chem. Res. Toxicol.* **2004**, *17*, 1399.
9. Ganley, B.; Chowdhury, G.; Bhansali, J.; Daniels, J. S.; Gates, K. S. *Bioorg. Med. Chem.* **2001**, *9*, 2395.
10. Azqueta, A.; Arbillaga, L.; Pachon, G.; Cascante, M.; Creppy, E. E.; Lopez de Cerain, A. *Chem. Biol. Interact.* **2007**, *168*, 95.
11. Azqueta, A.; Pachon, G.; Cascante, M.; Creppy, E. E.; de Cerain, A. L. *Mutagenesis* **2005**, *20*, 165.
12. Boiani, M.; Piacenza, L.; Hernández, P.; Boiani, L.; Cerecetto, H.; González, M.; Denicola, A. *Biochem. Pharmacol.* **2010**, *79*, 1736.
13. Cerecetto, H.; Di Maio, R.; González, M.; Risso, M.; Saenz, P.; Seoane, G.; Denicola, A.; Peluffo, G.; Quijano, C.; Olea-Azar, C. *J. Med. Chem.* **1999**, *42*, 1941.
14. Aguirre, G.; Cerecetto, H.; Di Maio, R.; González, M.; Alfaro, M. E. M.; Jaso, A.; Zarranz, B.; Ortega, M. A.; Aldana, I.; Monge-Vega, A. *Bioorg. Med. Chem. Lett.* **2004**, *14*, 3835.
15. Urquiola, C.; Vieites, M.; Aguirre, G.; Marín, A.; Solano, B.; Arrambide, G.; Noblia, P.; Lavaggi, M. L.; Torre, M. H.; González, M.; Monge, A.; Gambino, D.; Cerecetto, H. *Bioorg. Med. Chem.* **2006**, *14*, 5503.
16. Lavaggi, M. L.; Aguirre, G.; Boiani, L.; Orelli, L.; Garcia, B.; Cerecetto, H.; González, M. *Eur. J. Med. Chem.* **2008**, *43*, 1737.
17. Romeiro, N. C.; Aguirre, G.; Hernández, P.; González, M.; Cerecetto, H.; Aldana, I.; Pérez-Silanes, S.; Monge, A.; Barreiro, E. J.; Lima, L. M. *Bioorg. Med. Chem.* **2009**, *17*, 641.
18. Ancizu, S.; Moreno, E.; Torres, E.; Burguete, A.; Pérez-Silanes, S.; Benítez, D.; Villar, R.; Solano, B.; Marín, A.; Aldana, I.; Cerecetto, H.; González, M.; Monge, A. *Molecules* **2009**, *14*, 2256.
19. Boiani, M.; Cerecetto, H.; González, M.; Gasteiger, J. *J. Chem. Inf. Model.* **2008**, *48*, 213.
20. Vicente, E.; Charnaud, S.; Bongard, E.; Villar, R.; Burguete, A.; Solano, B.; Ancizu, S.; Pérez-Silanes, S.; Aldana, I.; Vivas, L.; Monge, A. *Molecules* **2008**, *13*, 69.
21. Vicente, E.; Lima, L. M.; Bongard, E.; Charnaud, S.; Villar, R.; Solano, B.; Burguete, A.; Pérez-Silanes, S.; Aldana, I.; Vivas, L.; Monge, A. *Eur. J. Med. Chem.* **2008**, *43*, 1903.
22. Vicente, E.; Pérez-Silanes, S.; Lima, L. M.; Ancizu, S.; Burguete, A.; Solano, B.; Villar, R.; Aldana, I.; Monge, A. *Bioorg. Med. Chem.* **2009**, *17*, 385.
23. Haddadin, M. J.; Issidorides, C. H. *Heterocycles* **1993**, *35*, 1503.
24. Cerecetto, H.; Di Maio, R.; Ibarruri, G.; Seoane, G.; Denicola, A.; Peluffo, G.; Quijano, C.; Paulino, M. *Farmaco* **1998**, *53*, 89.
25. Almeida-de-Faria, M.; Freymuller, E.; Colli, W.; Alves, M. J. M. *Exp. Parasitol.* **1999**, *92*, 263.
26. Faucher, J. F.; Baltz, T.; Petry, K. G. *Parasitol. Res.* **1995**, *81*, 441.
27. Boiani, L.; Davies, C.; Arredondo, C.; Porcal, W.; Merlino, A.; Gerpe, A.; Boiani, M.; Pacheco, J. P.; Basombrio, M. A.; Cerecetto, H.; Gonzalez, M. *Eur. J. Med. Chem.* **2008**, *43*, 2229.
28. Boiani, L.; Gerpe, A.; Aran, V. J.; de Ortiz, S. T.; Serna, E.; de Bilbao, N. V.; Sanabria, L.; Yaluff, G.; Nakayama, H.; de Arias, A. R.; Maya, J. D.; Morello, J. A.; Cerecetto, H.; Gonzalez, M. *Eur. J. Med. Chem.* **2009**, *44*, 1034.
29. Boiani, M.; Boiani, L.; Denicola, A.; de Ortiz, S. T.; Serna, E.; de Bilbao, N. V.; Sanabria, L.; Yaluff, G.; Nakayama, H.; de Arias, A. R.; Vega, C.; Rolan, M.; Gomez-Barrio, A.; Cerecetto, H.; Gonzalez, M. *J. Med. Chem.* **2006**, *49*, 3215.
30. Porcal, W.; Hernandez, P.; Boiani, M.; Aguirre, G.; Boiani, L.; Chidichimo, A.; Cazzulo, J. J.; Campillo, N. E.; Paez, J. A.; Castro, A.; Krauth-Siegel, R. L.; Davies, C.; Basombrio, M. A.; Gonzalez, M.; Cerecetto, H. *J. Med. Chem.* **2007**, *50*, 6004.
31. Moriguchi, I.; Hirono, S.; Liu, Q.; Nakagome, I.; Matshusita, Y. *Chem. Pharm. Bull.* **1992**, *40*, 127.
32. Hansch, C.; Leo, A. In *Exploring QSAR Fundamentals and Applications in Chemistry and Biology*; American Chemical Society: Washington, DC, 1995.
33. Katritzky, A. R.; Lobanov, V. S.; Karelson, M. *Chem. Soc. Rev.* **1995**, *24*, 279.
34. DRAGON 5.0 Evaluation Version. Available from: <http://www.disat.unimib.it/chm/>.
35. Akaike, H. Information Theory and Extension of the Maximum Likelihood Principle. In *Second International Symposium on Information Theory*; Petrov, B. N., Csáki, F., Eds.; Akademiai Kiado: Budapest, 1973; p 267.
36. Bader, R. F. W. In *Atoms in Molecules—A Quantum Theory*; Clarendon Press: Oxford, 1990.
37. Trinajstic, N. In *Chemical Graph Theory*; CRC Press: Boca Raton, FL, 1992.
38. Duchowicz, P. R.; Castro, E. A.; Fernandez, F. M.; Gonzalez, M. P. *Chem. Phys. Lett.* **2005**, *412*, 376.
39. Duchowicz, P. R.; Castro, E. A.; Fernández, F. M. *MATCH Commun. Math. Comput. Chem.* **2006**, *55*, 179.
40. Kubinyi, H. *Quant. Struct.-Act. Relat.* **1994**, *13*, 393.
41. Golbraikh, A.; Tropsha, A. *J. Mol. Graphics Modell.* **2002**, *20*, 269.
42. Hawkins, D. M.; Basak, S. C.; Mills, D. *J. Chem. Inf. Comput. Sci.* **2003**, *43*, 579.
43. Wold, S.; Eriksson, L. Statistical Validation of QSAR Results. In *Chemometrics Methods in Molecular Design*; van de Waterbeemd, H., Ed.; VCH: Weinheim, 1995; p 309.
44. Todeschini, R.; Consonni, V.. In *Molecular Descriptors for Chemoinformatics*; Wiley-VCH: Weinheim, 2009; Vol. 2,.
45. Table S1, including in Supporting Information, shows the predicted biological data of new proposed 3-arylquinoxaline di-*N*-oxides, **24**–**72**, according to QSAR equations 2 and 4.